Number 29
June 2006

SWISS NEUTRON NEWS

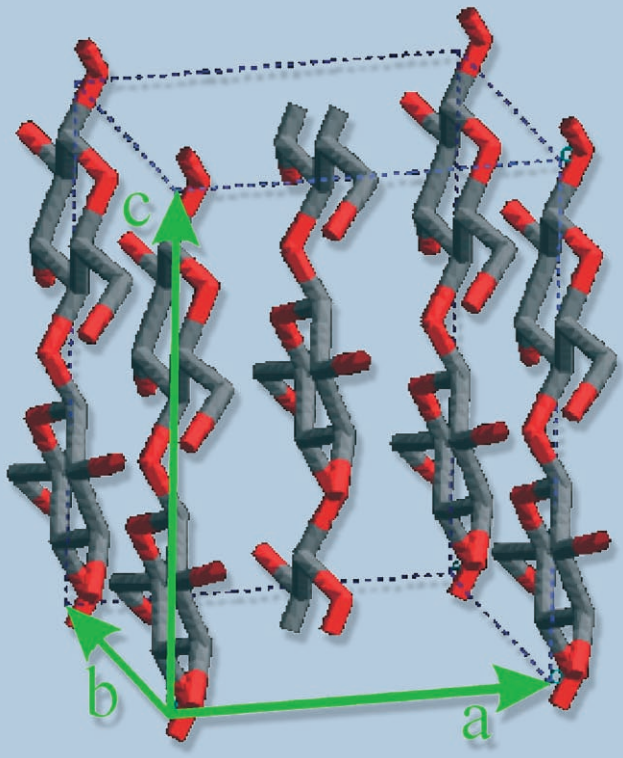

SSDN
SGN

Schweizerische Gesellschaft für Neutronenstreuung
Société Suisse pour la Diffusion des Neutrons
Swiss Neutron Scattering Society

Editorial

Editor: Swiss Neutron Scattering Society

Board for the Period January 2004 - January 2007:

President:	Dr. P. Allenspach	peter.allenspach@psi.ch
Board Members:	Prof. Dr. S. Decurtins	silvio.decurtins@iac.unibe.ch
	Prof. Dr. B. Schönfeld	schoenfeld@iap.phys.ethz.ch
Secretary:	Dr. S. Janssen	stefan.janssen@psi.ch

Honorary Members: Prof. Dr. W. Hälg, ETH Zürich
Prof. Dr. K.A. Müller, IBM Rüschlikon and Univ. Zürich
Prof. Dr. A. Furrer, ETH Zürich and Paul Scherrer Institut

Auditors: Dr. W. Fischer, Paul Scherrer Institut
Dr. K. Krämer, University of Berne

Address: Sekretariat SGN/SSDN
Paul Scherrer Institut
bldg. WLGA/002
5232 Villigen PSI, Switzerland
phone: +41-(0)56 - 310 4666
fax: +41-(0)56 - 310 3294
www: http://sgn.web.psi.ch

Bank Account: Postfinance: 50-70723-6 (BIC : POFICHBE)
IBAN: CH3909000000050707236

Printing: Paul Scherrer Institut

Circulation: 2000, 2 numbers per year

On the cover:

Unit cell of cellulose crystal type I_β. The carbon atoms are given in grey and the oxygen atoms in red. The fundamental vectors of the unit cell a, b, c are shown in green (see corresponding article on 'Host-Guest Interactions between Cellulose and Water' in this issue, page 29).

Contents

page

The President's Page

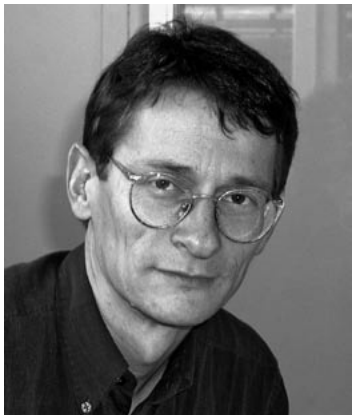

Dear members

On April 28, the first neutrons were produced at the first third generation neutron source SNS in Oak Ridge, USA. Congratulations to our friends in America! It is worth noticing that this project was realized well within schedule and budget, hence, it should serve as an example for other large-scale projects. The first three instruments (backscattering and two reflectometers) have started their commissioning phase but there is still a lot of work ahead until normal user operation can begin. However, you should slowly start to think about experiments at SNS. The Swiss 16T-magnet for SNS should be available for such experiments in about 2.5 years time, since the contract is – besides some technicalities – ready to be signed now.

The news from ESS is also kind of encouraging, since "The European Strategy Forum on Research Infrastructures" (ESFRI) will present a roadmap for European research infrastructures and both, the ESS project and the ILL millennium program, are identified as the two main neutron programs in Europe. ESS with its planned 5 MW long pulse target will be complementary to SNS, J-PARC and ISIS, however the design of well-adapted instruments is a challenge. There exists now a list of instrument groups, which will be refined during a meeting in September where instrument scientists and people who perform simulations will work closely together. Recently, the UK added another document in this context for a further discussion about the strategy for neutron sources from the UK perspective: "Future Access to Neutron Facilities: A Strategy for the UK" which can be downloaded at: http://www.neutrons.cclrc.ac.uk/.

The new liquid metal target MEGAPIE for SINQ has made good progress in the meantime and is expected to accept protons by July 24. Full power operation is scheduled for the end of July and a regular user cycle will start 1st of September and will last till Christmas. The neutron flux gain is expected to be 40 % compared to the normal steel clad solid lead target. In case MAGAPIE was not working properly or the experiment had to be discontinued for technical or safety reasons, it would take of the order of six weeks to replace it by a normal solid state target. This would of course cut

into the user beam time, but despite all these uncertainties, PSI was overwhelmed by the number of proposals for this fall cycle. With more than 160 proposals, almost twice as many were received as on average. Accordingly, the overbooking was in the range of 3 for each instrument.

As will be mentioned in this issue of neutron news, members of the Swiss Neutron Scattering Society can now pay their member fee of CHF 10/year also via wire transfer. We hope that this will make it easier to transfer this very modest amount and that this will increase our income from member fees (presently only 30 % pay their due). You can also transfer the membership fee for several years in advance in order to save on the transfer charges. If not specially earmarked as sponsoring, a larger amount transferred than CHF 10 will be assumed to be a multi years payment. We already thank you now for your contribution.

Peter Allenspach

Minutes of the SGN/SSDN General Assembly on May 10, 2006

Date/Locality: May 10, 2006, Paul Scherrer Institute, WHGA/001
Begin: 18:20
End: 19:07
Participants: 20 members of the society, 2 non-members

1. Welcome

The president of the SGN/SSDN, Peter Allenspach welcomes the participants to the general assembly 2006. In particular he welcomes the honorary member Albert Furrer.

2. Minutes of the General Assembly 2005

The minutes of the general assembly of the SGN/SSDN from January 27, 2005 published in Swiss Neutron News 27 (June 2005) are accepted without objections.

3. Annual Report of the Chairman

P. Allenspach reports on the activities of the SGN/SSDN in the year 2005:

a) In October 2005 the European Neutron Scattering Association ENSA awarded the prestigious Walter Hälg Prize jointly to the two society members Hans Ulrich Güdel and Albert Furrer. P. Allenspach congratulates both prize winners cordially on behalf of the SGN.

b) The SGN continued its activities regarding the supply of a 16T self-shielding magnet for the instruments of the SNS in Oak Ridge. The contract is expected to be signed by the end of May 2006. The magnet will be operational by the end of 2008 and the return for the Swiss neutron scattering community will be granted access to the instrumentation at SNS.

c) A welcome reception was offered by the society during the "PSI Summer School on Condensed Matter Research 2005" in Zuoz.

d) Two new issues of "Swiss Neutron News" were published, numbers 27 and 28, both issues are on the web: http://sgn.web.psi.ch/sgn/snn.html

e) Presently the society has 199 members.

f) The SGN now offers online registration for new members via the PSI Digital User Office Web-Interface. The registration form is available from the SGN Homepage: http://sgn.web.psi.ch

4. Report of the Treasurer

S. Janssen presents the annual balance sheet 2005:

Assets SGN/SSDN on 1.1.2005: **SFr 4931,90**

	Revenues [SFr]	**Expensens [SFr]**
Membership-fees (cash box)	260,–	
Membership-fees (postal check acc.)	330,–	
Donations (cash box)	30,–	
Total expenses		721,80
– Apéro Zuoz (2005)		690,–
– Expenses PC account		31,80
Credit for accrued interest	3,25	
Total	623,25	721,80
Net earnings 2004:		**– 98,55**
Assests SGN/SSDN on 31.12.2004:		**4833,35**

Balance sheet 2005:

	Assets [SFr]	**Liabilities [SFr]**
Postal check account	3581,45	
Cash box	1251,90	
Assets on 31.12.05	**4833,35**	

5. Report of the Auditors

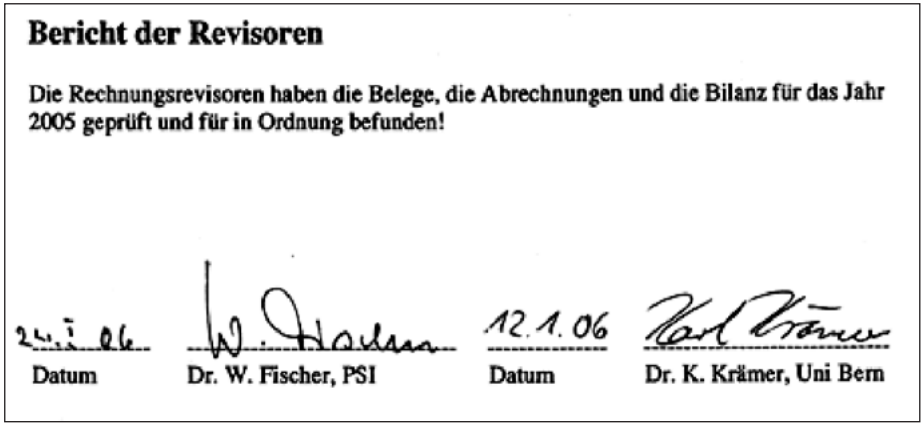

Bericht der Revisoren

Die Rechnungsrevisoren haben die Belege, die Abrechnungen und die Bilanz für das Jahr 2005 geprüft und für in Ordnung befunden!

24.1.06 — Datum — Dr. W. Fischer, PSI

12.1.06 — Datum — Dr. K. Krämer, Uni Bern

Both Auditors (W. Fischer, K. Krämer) have examined the bookkeeping and the balance 2005. They accepted it without any objections. The participants therefore unanimously vote for a release of the SGN/SSDN board.

W. Fischer claims the low total amount of member fees in 2005 and hopes that measures can be taken to increase the amount of accumulated fees in the future.

6. Budget 2006

The treasurer presents the following proposal for the budget 2006:

	Receipts [SFr]	**Expenditures [SFr]**
member fees	800,–	
interests	5,–	
fees PC account		40,–
Zuoz Apero 2006		600,–
Present HU Güdel		100,–
Total	805,–	740,–
balance 2006	**+ 65,-**	

The participants accept the budget proposal unanimously.

7. News from ENSA

P. Allenspach reports on recent news from the European Neutron Scattering Organization ENSA:

a) The European Science Foundation ESF will soon print the ENSA user survey.

b) K. Clausen reports briefly on some recent initiatives which have been launched to promote the ESS project:
   a. The European Strategy Forum on Research infrastructures (ESFRI) will present a roadmap for European Research infrastructures. Both the ESS project and the ILL millennium program are identified as the two main neutron programs in Europe. A. Furrer adds that the ESFRI expert group (which he is part of) is very positive about ESS.
   b. A 5MW long pulse design layout is clearly considered to be the most attractive one by ESFRI to be complementary to the SNS in Oak Ridge.
   c. Four candidate countries are identified to host ESS: Spain, Hungary, United Kingdom and Sweden, where the latter one seems to be mostly advanced with respect to funding negotiations and support by local governments.

c) During the last ENSA meeting H. Rauch/Vienna came up with a neutron scattering literature survey, which is briefly presented by P. Allenspach. The document compares the number of publications from different national neutron scattering communities and the respective number of citations. The following discussion among the participants can be summarized as follows:
   a. The SGN would welcome the creation of a publication database of European neutron scattering literature if that is feasible.
   b. Rather than comparing the output of different European countries it is of more interest to compare the output of various continental user groups (e.g. North America, Asia, Europe) and also to compare different methods (e.g. neutron scattering and NMR).

8. News from the Institute Laue Langevin, ILL

The share of beamtime for Swiss researchers at ILL was 3.18 % which is within the range of the long term average.

H. Schober reports on recent news from ILL:

a) The ILL welcomes Sweden, Hungary and Belgium as new scientific members

b) The strategy project “ILL 20/20” has been submitted to ESFRI

c) Personell: Richard Wagner replaced Werner Press as German Associate director. He will also act as General ILL director from October 1st. Andrew Harrison will become new British Associate director.

d) The REFIT-program (earthquake protection, reinforcement of buildings, reactor, guide hall, ILL4) is well on track. The restart of the reactor is scheduled for June 15. For 2006 three operation cycles are scheduled and four cycles with 56 days of neutron production each are foreseen from 2007 onwards.

e) New Infrastructures: The new guides for guide hall 7 are under installation and neutron guides with damaged Borofloat are being replaced. A new building with a Deuteration facility has been inaugurated. Furthermore an ILL-ESRF partnership in the field of Soft Condensed Matter has been proposed and waits for approval by the ILL and ESRF councils.

f) Millennium Program: Several projects could be completed like SALSA, D19, Flat Cone. Ongoing projects are: D3c, IN5, multiplexing TAS, LADI3, FIGARO, IN16B. Also new projects have been started like D11 detectors, PASTIS and DRACULA.

g) Long term strategy: A staged program based on review has been proposed. In a phase 1 (until 2011) the guide halls should be prepared for the installation of a third cold source and new guides H5 and H12 should be installed for the instruments PASTIS, DRACULA, IN14, WASP and D33. In a second phase (from 2011 on) the third cold source should be installed. ILL and ESRF then aim for the availability of high magnetic fields. Special attention will be paid to TAS and DIFF/TOF machines, new cold neutron instruments (LASI4, D44) and a new ultra cold neutron source.

h) On April 27-29 a very successful ILL Millennium Symposium was organized. H. Schober in particular emphasizes the strong and fruitful Swiss contributions.

A. Furrer remarks that the plans for the future ILL programs have been very positively received by the ESFRI neutron expert group.

9. Activities of the SGN/SSDN 2006

P. Allenspach informs briefly about the planned activities of the society in 2006:

a) The project of the Swiss SNS participation will be continued.

b) The SGN will apply for a membership of the Swiss Academy of Sciences. A first initiative has already been taken by A. Furrer a couple of years ago. At that time the SGN proposal was refused due to the interdisciplinary of the field “neutron scattering”. Now the Academy changed its priorities more towards interdisciplinary sciences and a new proposal will be launched.

c) As in the previous years the society will again sponsor a ‘welcome reception’ during the next ‘PSI Summer School on Condensed Matter Physics’ in Zuoz from

19-26/08/2006. The topic of the school 2006 will be 'Neutron, X-ray and Muon Studies of Nano Scale Structures' and the school will be organized by the NUM department of PSI.

10. Elections (see also Addendum 1)

This year elections for the Swiss representatives in the ILL colleges are necessary. F. Scheffold continues to represent the Swiss user community in college 9 (soft condensed matter) but successors for J. Mesot (college 4, excitations) and P. Allenspach (college 7, structural excitations) must be elected. With that respect the chairman thanks J. Mesot for his huge effort over the last years in the ILL college.

P. Allenspach proposes that due to the change of the ILL keywords Switzerland elects a representative for college 5B (magnetic structures) rather than college 7. He explains that he already contacted the ILL director C. Vettier in advance to discuss this issue and received a positive feedback. The participants unanimously accept this proposal.

He then proposes two candidates: B. Roessli (for college 4) and M. Medarde for college 5B. He briefly summarizes their CV and emphasizes that both are very experienced in their fields and spent a significant part of their scientific career at the ILL. Since there are no further candidates proposed by the participants he asks for a vote per acclamation.

Both candidates are unanimously accepted by the participants and accepted to represent the Swiss user community in the ILL colleges as described above. P. Allenspach will now forward the result of the election to the "Schweizer Staatssekretariat für Bildung und Forschung".

11. Miscellaneous

P. Allenspach informs the participants about two events in the next months:

a)Colloquium on the occasion of the retirement of Prof Hans-Ulrich Güdel on July 7, 2006, University of Berne, lecture hall EG16, time: 14:00

b)International Workshop on Advanced Monte Carlo Simulations in Neutron Scattering, October 2-4, 2006, Paul Scherrer Institute: http://lns00.psi.ch/mcworkshop/

S. Janssen, SGN secretary

May 15, 2006

Addendum 1 (June 26, 2006)

On June 23 the ILL invited E. Lehmann from the PSI Neutron Imaging group via the "Schweizer Staatssekretariat für Bildung und Forschung" to join ILL subcommittee 1. P. Allenspach forwarded the request to E. Lehmann. He accepted to join subcommittee 1, such that Switzerland now sends four representatives to the ILL subcommittees.

Interstitial oxygen in lanthanum oxy-apatite electrolytes for SOFC

*L. León-Reina[1], J.M. Porras-Vázquez[1], E.R. Losilla[1], M. Martínez-Lara[1], S. Bruque[1], D. Sheptyakov[2], M.A.G. Aranda[1]**

[1]Dept. Química Inorgánica, Universidad de Málaga, Campus Teatinos, 29071-Málaga, Spain
[2]Laboratory for Neutron Scattering, Paul Scherrer Institut & ETH Zürich, 5232 Villigen PSI, Switzerland
** To whom the correspondence should be addressed: g_aranda@uma.es*

Abstract

Rare earth oxy-apatites are attracting considerable interest as electrolytes for solid oxide fuel cell (SOFC) due to their high oxide ion conductivities and low activation energies. The oxide conductivities are comparable and sometimes even higher than those of Yttria-Stabilized-Zirconia (YSZ). Several oxy-apatites materials including $La_{9.33}\square_{0.67}(Si_6O_{24})O_2$, $La_{9.50}\square_{0.50}(Si_{5.5}Al_{0.5}O_{24})O_2$, $La_8Sr_2(Si_6O_{24})O_2$, $La_8Sr_2(Ge_6O_{24})O_2$, $La_{9.55}\square_{0.45}(Si_6O_{24})O_{2.32}$, $La_{9.60}\square_{0.40}(Ge_6O_{24})O_{2.40}$, and $La_{9.75}\square_{0.25}(Ge_6O_{24})O_{2.62}$ have been prepared as crystalline phases and characterized by electrochemical techniques. A thorough study, using neutron powder diffraction (NPD) and the Rietveld method, has been carried out to analyze the oxygen sublattices. Firstly, we have found interstitial oxide anions in addition to the oxides at the center of the apatite channels for some compositions that displayed the highest conductivities. Furthermore, the interstitial oxide position in oxygen-excess silicates without vacancies in the lanthanum sublattice, f. i. $La_{8.65}Sr_{1.35}(Si_6O_{24})O_{2.32}$, is different from that in germanates, f. i. $La_{8.65}Sr_{1.35}(Ge_6O_{24})O_{2.32}$. This is likely due to the different structural flexibility of the two tetrahedral groups and it explains the previously reported feature of higher oxygen contents for germanates oxy-apatites. Secondly, the complementary use of synchrotron X-ray powder diffraction (SXRPD) has showed that germanium apatites are hexagonal (s.g. $P6_3/m$) for ion oxide contents lower than 2.4 and triclinic (s.g. $P\bar{1}$) for higher oxide contents. Conversely, silicon oxy-apatites are hexagonal for all compositions. The structural characteristics of these oxide anion conductors are discussed.

Introduction

Research on oxy-apatites [1,2] has grown following the exciting reports by Nakayama et al. [3,4] about high oxide conductivities in rare earth silicates, $Ln_{10}(Si_6O_{24})O_3$ with oxy-apatite structure. Many materials crystallize in this well known structure-type

with structural formula $A_{10}(TO_4)_6X_2$ where A is generally a large divalent cation (Ca^{2+}, Sr^{2+}, Pb^{2+}, Cd^{2+}, etc.), TO_4 is a tetrahedral anionic group (PO_4^{3-}, VO_4^{3-}, AsO_4^{3-}, etc.) and X is a monovalent anion (F^-, OH^-, etc.). Concerning the oxide ion conductivity, the best properties have been observed in oxy-apatites, where $X=O^{2-}$, T=Si/Ge and A corresponds to rare earth cations. The initials works on oxy-apatite conductors were focused on $Ln_{10-(1-x)2/3}\square_{(1-x)2/3}(Si_6O_{24})O_{2+x}$ systems, these phases have been prepared as polycrystalline powder (by standard solid state techniques [5] and sol-gel synthesis [6]) and/or single crystals by the floating zone method [7]. There have also been several studies with Ge, and the $La_{10-(1-x)2/3}\square_{(1-x)2/3}(Ge_6O_{24})O_{2+x}$ series has been studied by NPD and SXRPD and impedance spectroscopy [8]. Mixed Ge-Si oxy-apatites [9] and derivatives [10] are also known. There are other related compounds with the same framework, but with atomic substitutions at the A and T site [1], some including transition metals [11]. For example, the conductivity of $La_{10-(1-x)2/3}\square_{(1-x)2/3}(T_6O_{24})O_{2+x}$ (T=Si and Ge) has been enhanced by partial substitution of Si/Ge by Al [12,13]. Some important experimental contributions to the knowledge of the relationship between structure and oxide conductivity are those works using NPD [8,13-16].

There are two paradigmatic rare earth oxy-apatites, $La_{9.33}\square_{0.67}(SiO_4)_6O_2$ and $La_8Sr_2(SiO_4)_6O_2$. $La_{9.33}\square_{0.67}(SiO_4)_6O_2$ has an oxide conductivity almost three orders of magnitude larger than that of $La_8Sr_2(SiO_4)_6O_2$ and their mechanistic features of oxygen ion transport at atomic level have been recently studied [17,18] using computer modelling techniques. These studies found a subtle but conspicuous difference between $La_{9.33}\square_{0.67}(SiO_4)_6O_2$ and $La_8Sr_2(SiO_4)_6O_2$. The atomistic modelling proposed that the high ionic conductivity and low activation energy of $La_{9.33}\square_{0.67}(SiO_4)_6O_2$ is due to an interstitial oxygen mechanism, where oxygen migration takes place along the c-axis via a sinusoidal-like pathway. However, the computer modelling gave no interstitial oxygen in $La_8Sr_2(SiO_4)_6O_2$. The merit of this atomistic simulation approach is that it models the local lattice relaxation around the migrating oxygen ion.

As part of our ongoing research on electrolytes for SOFC, we have carried out a systematic investigation to characterize the presence of interstitial oxygen in oxygen-stoichiometric and oxygen excess apatites. These materials may or may not have vacancies at the lanthanum sublattice. In this paper, we report a summary of the crystallochemical features of oxy-apatites and their relationships with the oxide conductivity.

Experimental

Oxy-apatites were prepared by solid state reactions and synthetic details may be found elsewhere [8,13-16]. The compositions studied by constant wavelength NPD were: $La_{9.33}\square_{0.67}(Si_6O_{24})O_2$, $La_{9.50}\square_{0.50}(Si_{5.5}Al_{0.5}O_{24})O_2$, $La_{9.50}\square_{0.50}(Ge_{5.5}Al_{0.5}O_{24})O_2$, $La_{9.55}\square_{0.45}(Si_6O_{24})O_{2.32}$, $La_{9.60}\square_{0.40}(Ge_6O_{24})O_{2.4}$, $La_{9.75}\square_{0.25}(Ge_6O_{24})O_{2.62}$, $La_{8.65}Sr_{1.35}(Si_6O_{24})O_{2.32}$, $La_{8.65}Sr_{1.35}(Ge_6O_{24})O_{2.32}$ and $La_9Sr_1(Si_{5.5}Al_{0.5}O_{24})O_{2.25}$. The

patterns were taken at RT and high-temperature (773 K and 1173 K) on HRPT diffractometer [SINQ neutron source, at Paul Scherrer Institut, Villigen, Switzerland] with the samples loaded in vanadium cans. The neutron wavelength, usually 1.886 Å, was selected by the (511) reflection of the vertically-focusing Ge monochromator. The overall measuring time was ≈6 h per pattern to have good statistics over the 2θ angular range of 5–165° [21–0.95Å] with 0.05º step size.

Time-of-flight (tof)-NPD data were taken for $La_{9.33}\square_{0.67}(Si_3Ge_3O_{24})O_2$, $La_8Sr_2(Si_6O_{24})O_2$ and $La_8Sr_2(Ge_6O_{24})O_2$ at 300K on HIPD diffractometer [Lujan Neutron Scattering Center, LANSCE, Los Alamos, USA]. Data from the two detector banks with highest resolution (±153º) were used for the Rietveld refinements [19]. Data were collected during 2 h and normalized by the incident spectrum. The analyzed neutron data range was 2 to 20 ms which corresponds to 0.4-4 Å in d-spacings.

High resolution SXRPD patterns at room temperature were collected on ID31 diffractometer [European Synchrotron Radiation Facility (ESRF), Grenoble, France] for $La_{9.60}\square_{0.40}(Ge_6O_{24})O_{2.4}$, $La_{9.75}\square_{0.25}(Ge_6O_{24})O_{2.62}$, $La_{8.65}Sr_{1.35}(Si_6O_{24})O_{2.32}$ and $La_{8.65}Sr_{1.35}(Ge_6O_{24})O_{2.32}$. The samples were loaded in a borosilicate glass capillary (ϕ = 1 mm) and rotated during data collection. A penetrating wavelength, λ = 0.40 Å (31 keV), was selected with a double-crystal Si (111) monochromator and calibrated with Si standard from NIST (a = 5.431195 Å). The overall measuring time was ≈1 h to have very good statistics over the angular range 2-30° (in 2θ) [11.5-0.77Å]. The data from the multi-analyzer Si(111) stage were normalized and summed up to 0.003º step size with local software to produce the final raw data.

Results and discussion

Oxygen stoichiometric oxy-apatites

We have investigated the presence of interstitial oxygen in oxygen stoichiometric samples (associated to oxygen vacancies at the channel sites). These compounds may have or may have not vacancies at the lanthanum sublattice. The oxygen stoichiometric samples with vacancies at the lanthanum sublattice studied by NPD were: $La_{9.33}\square_{0.67}(Si_6O_{24})O_2$, $La_{9.33}\square_{0.67}(Si_3Ge_3O_{24})O_2$, $La_{9.50}\square_{0.50}(Si_{5.5}Al\text{-}O_{24})O_2$ and $La_{9.50}\square_{0.50}(Ge_{5.5}Al_{0.5}O_{24})O_2$. The results have been already reported [13-16] and the presence of interstitial oxygen was confirmed at the position theoretically predicted by atomistic simulations [17,18] for $La_{9.33}\square_{0.67}(Si_6O_{24})O_2$. The position of the interstitial oxide anions, O(5), see Figure 1a, is very close to the average position of one oxygen of a tetrahedral group, O(3) [1.1 Å] but the atomistic calculations showed that the lattice can accommodate it through a local relaxation. The oxygen stoichiometric samples without vacancies at the lanthanum sublattice investigated by NPD were: $La_8Sr_2(Si_6O_{24})O_2$ and $La_8Sr_2(Ge_6O_{24})O_2$. The joint X-ray and neutron powder diffrac-

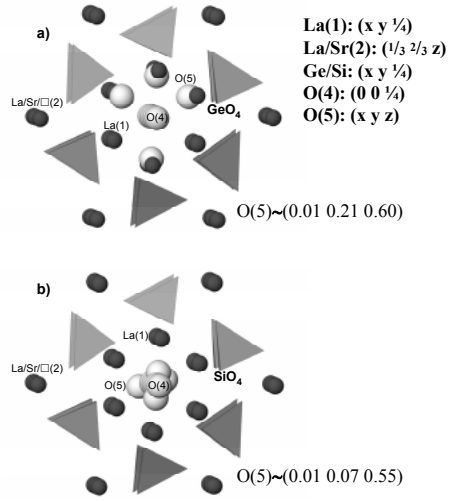

Figure 1: c-axis view of the crystal structure of a) $La_{8.65}Sr_{1.35}(Ge_6O_{24})O_{2.32}$ and b) $La_{8.65}Sr_{1.35}(Si_6O_{24})O_{2.32}$, showing the TO_4 groups as tetrahedra and La(1), La/Sr(2) and O(4) atom as balls. The cation vacancies are not shown. Interstitial oxygen, O(5), is highlighted (white-grated balls) and shown at 16 % of occupancy for clarity.

tion Rietveld refinements gave no interstitial oxygens [15] also in agreement with the theoretical calculations. Hence, we can conclude that the samples with highest oxide conductivities are those with lanthanum vacancies because they stabilize the presence of interstitial oxide anions which have higher mobilities and lower activation energies.

The interstitial oxide anions, O(5), are roughly located at the periphery of the oxide channels, O(4) see Figure 1a, close to La(1) atoms and TO_4 tetrahedra with occupation factors ranging between 1-4 %. The local environment around O(5) can not be obtained by diffraction methods as these methods yield an average structure dominated by the non-relaxed fraction of the framework (94-99 % of the structure). The average O(5)···O(3) distance, ~1.1 Å, has non crystallochemical meaning and the real oxygen separation is much large because the local lattice relaxation close to the interstitial oxides. This relaxation is a rotation and translation of the $Si(Ge)O_4$ tetrahedron towards the La(2) vacancies. The increasing of some anisotropic thermal coefficients is an indirect evidence of this relaxation. In fact, the reported anisotropic thermal parameters take into account, not only the thermal vibration, but also a very important contribution from the local lattice distortion in the vicinity of the interstitial oxygen. The main parameter to detect this relaxation is U_{11} of O(3), it reflects the local movement of some of these atoms. As it can be seen in previous publications [8,13-16], O(3) is significantly more disordered in the samples with interstitial oxide anions.

Oxygen excess oxy-apatites

We have also investigated the presence and location of interstitial oxygen in oxygen-excess samples. Initially, we carried out a high-resolution SXRPD study for $La_{9.60}\square_{0.40}(Ge_6O_{24})O_{2.4}$, $La_{9.75}\square_{0.25}(Ge_6O_{24})O_{2.62}$, $La_{8.65}Sr_{1.35}(Si_6O_{24})O_{2.32}$ and $La_{8.65}Sr_{1.35}(Ge_6O_{24})O_{2.32}$. The synchrotron pattern for $La_{9.60}\square_{0.40}(Ge_6O_{24})O_{2.4}$, $La_{8.65}Sr_{1.35}(Si_6O_{24})O_{2.32}$ and $La_{8.65}Sr_{1.35}(Ge_6O_{24})O_{2.32}$ showed anisotropic broadening

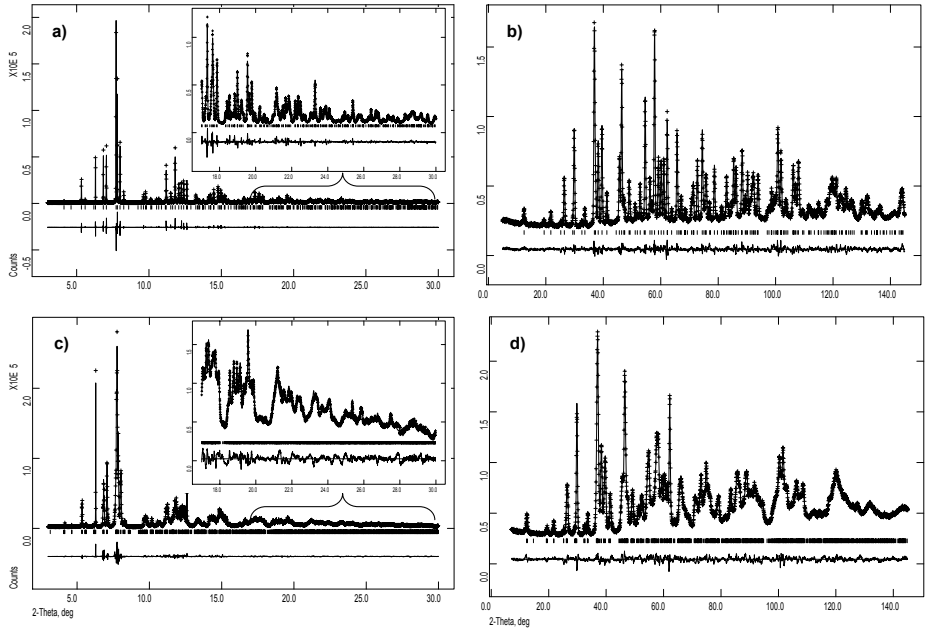

Figure 2: Observed (crosses), calculated (full line) and difference (bottom) Rietveld patterns for $La_{9.60}\square_{0.40}(Ge_6O_{24})O_{2.4}$: a) SXRPD data, b) NPD data; and $La_{9.75}\square_{0.25}(Ge_6O_{24})O_{2.62}$: c) SXRPD data, d) NPD data. The insets in the SXRPD plots enlarge the high-angle regions to highlight the differences between the hexagonal and triclinic patterns.

with asymmetric tails for some reflections. This is likely linked to the incommensurate diffuse spots observed for $La_{9.33}\square_{0.67}(Si_6O_{24})O_2$ by electron diffraction [20]. The procedure used to properly fit the highly anisotropic SXRPD peaks is described in detail elsewhere [8,16]. All peaks in the SXRPD patterns were accounted for with $P6_3/m$ symmetry. Many split peaks appeared in the SXRPD pattern for $La_{9.75}\square_{0.25}(Ge_6O_{24})O_{2.62}$ that could not be explained with the hexagonal symmetry. Hence, to satisfactorily fit the SXRPD patterns we lowered the symmetry to triclinic Pī which is a subgroup the hexagonal one. Figure 2 shows the Rietveld synchrotron and neutron plots for hexagonal $La_{9.60}\square_{0.40}(Ge_6O_{24})O_{2.4}$ and triclinic $La_{9.75}\square_{0.25}(Ge_6O_{24})O_{2.62}$. The triclinic oxyapatite structure is very complex but the NPD-SXRPD joint refinement has allowed to obtain a good structural description [8].

SXRPD data have shown that $La_{10-(1-x)2/3}\square_{(1-x)2/3}(Ge_6O_{24})O_{2+x}$ series is single phase in the ($0.18\leq x\leq 0.62$) compositional range being hexagonal (s.g. $P6_3/m$) for $0.18\leq x\leq 0.33$ and triclinic (s.g. Pī) for $0.33\leq x\leq 0.62$ [8]. On the other hand, $La_{10-(1-x)2/3}\square_{(1-x)2/3}(Si_6O_{24})O_{2+x}$ is single phase in the ($0\leq x\leq 0.40$) compositional range

and the symmetry is always hexagonal [14]. This different behavior is very likely due to the more flexible germanate tetrahedron which allows a higher amount of interstitial oxide anions distorting the structure to triclinic.

Now, we will focus on the presence and location of the interstitial oxygens for oxygen-excess samples, i.e. those with oxide anions content higher than 2.0. Two type of oxy-apatites can be distinguished: those with vacancies at the lanthanum sublattice, f. i. $La_{9.55}\square_{0.45}(Si_6O_{24})O_{2.32}$ and $La_{9.60}\square_{0.40}(Ge_6O_{24})O_{2.4}$; and those with full occupancy at the lanthanum sublattice, f. i. $La_{8.65}Sr_{1.35}(Si_6O_{24})O_{2.32}$, $La_{8.65}Sr_{1.35}(Ge_6O_{24})O_{2.32}$ and $La_9Sr_1(Si_{5.5}Al_{0.5}O_{24})O_{2.25}$. NPD has allowed to determine the position of the interstitial oxygen in these samples. For the first type of materials, these extra oxide anions are located in the same position reported above for the oxygen stoichiometric samples [14].

For $La_{8.65}Sr_{1.35}(Si_6O_{24})O_{2.32}$, $La_{8.65}Sr_{1.35}(Ge_6O_{24})O_{2.32}$ and $La_9Sr_1(Si_{5.5}Al_{0.5}O_{24})O_{2.25}$, the interstitial oxygen position depends upon the element on the tetrahedral sites [16]. Silicate samples have the extra-oxygen very close to the oxide channels (Figure 1b) but the germanate samples have the extra oxygens in the periphery of the oxide channels (Figure 1a) in a position very close to that described above for the oxygen-stoichiometric samples with vacancies at the lanthanum sublattice. For $La_{8.65}Sr_{1.35}(Si_6O_{24})O_{2.32}$, the average (not real) O(5)···O(4) and O(5)···O(3) distances are 1.54(3) and 2.37(2) Å, respectively. For La8.65Sr1.35(Ge6O24)O2.32, the average O(5)···O(4) and O(5)···O(3) distances are 2.33(1) and 1.15(2) Å, respectively (see Figure 1).

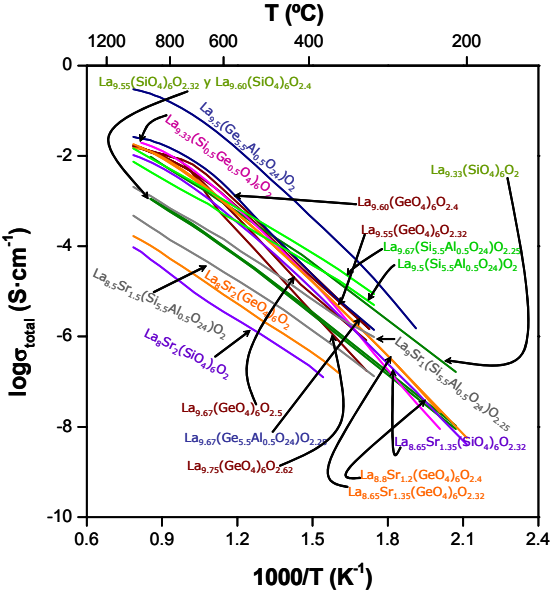

Figure 3: Arrhenius plot of $\log\sigma_{total}$ versus 1000/T for several compositions with the oxy-apatite type structure [21].

Formal inclusion of the interstitial oxygens at the channel periphery in diffraction data analysis is difficult because the stable interstitial site lies too close to other atoms (either an oxygen of the silicate substructure in $La_{8.65}Sr_{1.35}(Ge_6O_{24})O_{2.32}$ or the loosely bounded oxide of the center of the channels in $La_{8.65}Sr_{1.35}(Si_6O_{24})O_{2.32}$). This closeness (1.1-1.5 Å) requires local relaxation of the structure around the site, which is not possible to model accurately with diffraction methods as we have discussed above. However, some clues about the local relaxation can be indirectly extracted from the anisotropic atomic displacement parameters when studying a series in a consistent way as shown previously [13-16].

Conductivity study

Now, it starts to be clear that the oxide anion conductivities of lanthanum oxy-apatites are governed by three key parameters: a) the lanthanum vacancies, which allow the local lattice relaxation around the interstitial oxide anions, b) the amount and position of the interstitial oxide anions O(5), c) the amount of oxide vacancies at the channels, O(4). These parameters can be obtained by NPD and allow to explain the difference in conductivities by more than 5 orders in magnitude for different oxy-apatites (see Figure 3).

To conclude, the samples that display higher conductivities, so far, are those oxygen-stoichiometric but with vacancies at the lanthanum sublattice. These samples have interstitial oxygens O(5) associated with oxygen vacancies at the oxide channels, O(4).

Acknowledgments

The work in Málaga has been supported by the MAT2003-07483-C2-1 research grant. The neutron scattering research was performed at the spallation neutron source SINQ and at Lujan Center at Los Alamos National Laboratory under the Department of Energy-Basic Energy Sciences national user program. Los Alamos is operated by the University of California for the DOE Contract W-7405-ENG-36. ESRF is thanked for the provision of X-ray synchrotron facilities.

Bibliography

[1] P.R. Slater, J.E.H. Sansom, J.R.Tolchard, The Chem. Record 4 (2004) 373 (and references therein).

[2] V.V. Kharton, F.M.B. Marques, A. Atkinson, Solid State Ionics 174 (2004) 135.

[3] S. Nakayama, H. Aono, Y. Sadaoka, Chem. Lett. (1995) 431.

[4] S. Nakayama, M. Sakamoto, J. Eur. Ceram. Soc. 18 (1998) 1413.

[5] a) S. Tao, J.T.S. Irvine, Mater. Res. Bull. 36 (2001) 1245. b) P.R. Slater, J.E.H. Sansom, Solid State Phenomena 90-91 (2003) 195.

[6] a) S. Célérier, C. Laberty, F. Ansart, P. Lenormand, P. Stevens, Ceramics International 32 (2006) 271. b) Y. Masubuchi, M. Higuchi, T. Takeda, S. Kikkawa, Journal of Alloys and Compounds 408-412 (2006) 641.

[7] M. Higuchi, Y. Masubuchi, S. Nakayama, S. Kikkawa, K. Kodaira, Solid State Ionics 174 (2004) 73 and references therein.

[8] L. León-Reina, M.C. Martín-Sedeño, E.R. Losilla, A. Cabeza, M. Martínez-Lara, S. Bruque, F.M.B. Marques, D.V. Sheptyakov, M.A.G. Aranda, Chem. Mater. 15 (2003) 2099.

[9] J.E.H. Sansom, P.R. Slater, Solid State Ionics 167 (2004) 23.

[10] J.E.H. Sansom, P.A. Sermon, P.R. Slater, Solid State Ionics 176 (2005) 1765.

[11] a) H. Yoshioka, S. Tanase, Solid State Ionics 176 (2005) 2395. b) A.L. Shaula, V.V. Kharton, J.C. Waerenborgh, D.P. Rojas, F.M.B. Marques, J. Eur. Ceram. Soc. 25 (2005) 2583.

[12] E.J. Abram, D.C. Sinclair, A.R. West, J. Mater. Chem. 11 (2001) 1978.

[13] L. León-Reina, E.R. Losilla, M. Martínez-Lara, M.C. Martín-Sedeño, S. Bruque, P. Núñez, D.V. Sheptyakov, M.A.G. Aranda, Chem. Mater. 17 (2005) 596.

[14] L. León-Reina, E.R. Losilla, M. Martínez-Lara, S. Bruque, M.A.G. Aranda, J. Mater. Chem. 14 (2004) 1142.

[15] L. León-Reina, E.R. Losilla, M. Martínez-Lara, S. Bruque, A. Llobet, D.V. Sheptyakov, M.A.G. Aranda, J. Mater. Chem. 15 (2005) 2489.

[16] L. León-Reina, J.M. Porras-Vázquez, E.R. Losilla, M.A.G. Aranda, Solid State Ionics, submitted.

[17] M.S. Islam, J.R. Tolchard, P. R. Slater, Chem. Commun. (2003) 1486.

[18] J.R. Tolchard, M.S. Islam, P.R. Slater, J. Mater. Chem. 13 (2003) 1956.

[19] H.M. Rietveld, J. Appl. Crystallogr. 2 (1969) 65.

[20] P. Berastegui, S. Hull, F.J. García, J. Grins, J. Solid State Chem. 168 (2002) 294.

[21] L. León-Reina, Doctorate Thesis, Universidad de Málaga, Spain, 2005. Available as a CD from lauralr@uma.es or g_aranda@uma.es

Interface effects in $YBa_2Cu_2O_{7-\delta}$ / $La_{2/3}Ca_{1/3}MnO_3$ multilayers

J. Stahn[1], C. Niedermayer[1], J. Hoppler[2], C. Bernhard[2]

[1] Laboratory for Neutron Scattering, ETH Zürich & Paul Scherrer Institute
[2] Physics Department, University of Fribourg

Abstract

The profile of the magnetization in a multilayer of the high temperature superconductor YBCO and the ferromagnet LCMO has been investigated by polarized neutron reflectometry. Surprisingly, the YBCO layer shows a magnetic induction at its interfaces, with an antiferromagnetic coupling to the magnetization in the LCMO layer. This magnetic antiphase proximity effect sets in well below the Curie temperature of LCMO but still above the superconducting transition. As the YBCO layers enter the superconducting state, the size of the magnetic domains within the LCMO layer is significantly reduced.

New physics at interfaces?

One of the incentives of the increasingly important field of materials science concerned with the fabrication and characterization of multilayers, is the search for new or strongly modified physical properties at their interfaces which eventually allow for new technical applications. A well known example in this context is the discovery of the giant magnetoresistence (GMR) effect, nowadays used in all hard disk devices in the read heads.

The interesting interface properties may result from the close proximity of layer materials with competing or even exclusive physical properties. Lattice mismatch on the atomic scale between the layer materials can lead to strain and dislocations or to a complete reconstruction of the crystal structure. Chemical interdiffusion can alter the composition. Charge injection changes electronic states and thus eventually also magnetic properties. All these phenomena are restricted to the interface region and therefore new quasi 2-dimensional *materials* with properties different from the *bulk materials* may be formed.

In systems with more than two layers an additional effect may become important: the coupling of physical properties across a *spacer* layer. E.g. the ferro- or antiferromag-

netic alignment of ferromagnetic layers is determined by the spacer material and its thickness.

In this article we present our work on perovskite based superlattices consisting of the ferromagnet LCMO and the high-T_c superconductor YBCO.

From magnetization measurements at different external magnetic fields an unexpected increase of the magnetization below the onset of superconductivity was observed [1]. In order to determine the location of the magnetization within the multilayer low-energy muon spin rotation experiments were performed. Surprisingly, an increase of the internal magnetic field was not only observed, when the muons were implanted into the LCMO layer, but also when they are stopped within the YBCO layer. The spatial resolution of this technique is limited by the rather large energy dependent stopping distribution of a charged particle in matter, which for the experiment described above was of the order of the layer thickness itself (about 10 - 20 nm).

Under certain conditions polarized neutron reflectometry allows for the determination of in-plane magnetization with a depth resolution below 1 nm. One condition is an adequate design of the layer thicknesses, another one a sufficient contrast, both by the nuclei and the magnetization [2].

In recent years X-ray magnetic circular dichroism (XMCD) was developed to be a competitive method to PNR with the advantage of measuring element specific magnetic moments, but with the disadvantage of being restricted to regions close to the sample surface.

The combination of both methods allows for a very detailed reconstruction of the in-plane magnetic induction profile $B_{\|}(z)$. The PNR part is presented in the following, for the XMCD measurements please refer to the paper by Chakhalian and coworkers [3].

Epitaxial perovskite multilayers

An ideal playground for the investigation of interface effects and coupling phenomena is the family of perovskite type oxides. By varying the elements or element mixtures and by depleting the oxygen content it is possible to tailor materials, which are ferro-, antiferro- or paramagnetic, metallic, half-metallic or insulating. The fact that they all belong to the same crystal type with very similar lattice parameters allows for the growth of epitaxial superlattices with rather flat and sharp interfaces, which is fundamental for the research and for the application of the devices. Epitaxy in general means, that at least some symmetry elements are preserved during the sample growth. Here it means that the in-plane dimensions and often in-plane symmetry are not altered across the interface. Just the occupancy of the lattice sites changes (eventually leading

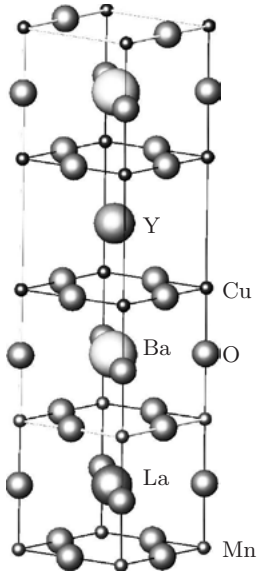

Figure 1: Atomic stacking sequence and arrangement of atoms at the YBCO / LCMO interface. The oxygen lattice is continous (with the exception of vacancies in the Y-planes), while the cations and the number of building blocks per cell change.

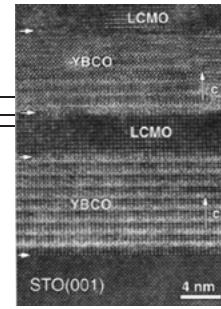

Figure 2: TEM image of a YBCO/LCMO multilayer [4]. The different materials with their characteristic unit cell dimensions are visible. The interfaces are atomically flat.

to multiplication of the unit cell) and the cell parameter out of plane (z-direction) might be altered to compensate for the strain due to in-plane mismatch.

High quality $La_{2/3}Ca_{1/3}MnO_3$ (LCMO) / $YBa_2Cu_2O_{7-\delta}$ YBCO multilayers were grown on $SrTiO_3$ (STO) by *Pulsed Laser Deposition (PLD)* at the MPI FKF in Stuttgart [4]. Fig. 1 shows the unit cells of LCMO and YBCO at the interface. A structural study using x-ray refinement and high-resolution transmission electron microscopy (Fig. 2) shows sharp interfaces with a high degree of structural perfection.

STO is widely used as a substrate material because it is a paramagnetic insulator not interacting with the layers on top, and because it is available in sufficient quality and size. A disadvantage of STO is its structural phase transition at about 110 K leading to strain and thus to a wavy surface.

Depending on the La to Ca ratio, LCMO exhibits different magnetic and conducting ground states. For $0.2 < x < 0.5$ the material is a ferromagnetic metal, which displays very large magnetoresistive effects termed collosal magneto resistance (CMR). The composition with x=0.33 has the highest Curie temperature $T_{Curie} \approx 260\ K$ for bulk material.

YBCO is a high-T_c superconductor with the transition temperature as high as $T_c \approx 92\ K$. For oxygen depletion T_c decreases *(underdoped regime)*. In our samples YBCO is slightly underdoped *($\delta \approx 0.1$)*.

The characteristic temperatures given above are for bulk material. In thin films (of the order of a few nm), the values are normally decreased, where the actual value in multilayers depends on both, the layer thickness and the periodicity.

For the reflectivity measurements we used samples with (almost) equally thick YBCO and LCMO films with bilayer thicknesses reaching from 20 nm to 50 nm. The number of periods was 5 to 16, depending on the thicknesses. The total thickness for our materials is restricted to about 300 nm due to the fact that thicker films fail to grow epitactically with sufficient quality.

Polarized neutron reflectometry

In reflectivity experiments the scattering vector **q** is close to normal to the flat surface of the sample (z-direction), the angle of incidence α_i is of the order of the angle of total external reflection α_c. The technique allows one to probe a potential profile normal to the surface ($\mathbf{q} = \mathbf{q}_z$, *specular* reflectivity) or lateral inhomogeneities ($\mathbf{q} = \mathbf{q}_z + \mathbf{q}_x$, *off-specular* reflectivity). For cold neutrons with wavelength $\lambda \approx 5$Å typical values are $0° < \alpha_i < 5°$ resulting in a spatial resolution as small as 1Å in z-direction and of the order of μm in x-direction (x and z are in the scattering plane, y is normal to it and in convential reflectometry experiments the intensity is integrated over $\mathbf{q}_y$). Scattering vector, angle of incidence α_i and wavelength λ are related by $q_z = 4\pi \sin(\alpha_i/\lambda)$. To measure the reflectivity $R(q_z)$ one can vary α_i at constant λ. An example for such an angle-dispersive set-up is given in Fig. 3. In an energy dispersive mode λ is varied while α_i is fixed. This mode is realized on the time-of-flight reflectometer AMOR.

The potential seen by the neutrons under reflectivity conditions is given by the laterally averaged nuclear and magnetic potentials:

$V = 2\pi\hbar^2/m \sum_i \rho_i b_i + \mu_n \mathbf{B}_\parallel$ with i running over all isotopes with number density ρ_i and scattering lengths b_i. μ_n is the neutron magnetic moment and $\mathbf{B}_\parallel$ the in-plane magnetic induction. Out-of-plane components of **B** do not contribute to the specular scattered intensity.

The measured quantity $R(q_z)$ is proportional to the number of neutrons reflected by a surface (Fresnel reflectivity). If several parallel interfaces are present $R(q_z)$ is the result of the interference of the Fresnel reflectivities of each interface. The phases are determined by the layer distances and the sign of the potential while the amplitudes are given by the height of the steps. As a first approximation (no refraction, no multiple scattering) $R(q_z)$ is proportional to the Fourier transform of $V(z)$ squared and therefore all phase information and thus the information on the order of the interfaces is lost.

To deduce a potential profile from $R(q_z)$ one has to calculate the reflectivity from a model profile, which after comparison with the measured data has to be refined. Generally there is no unique solution for a measured data set, but with the knowledge of

specific sample properties and additional information obtained by other techniques it is possible to exclude many (if not most) of the models.

Our measurements have been performed in an angle-dispersive mode on Morpheus@SINQ, ADAM@ILL and on HADAS@Jülich (wavelengths 4.4 to 4.8 Å); energy dispersive measurements were performed on AMOR@SINQ. We performed specular reflectivity measurements up to q_z = 0.1Å^{-1} with a rather poor resolution of $\Delta q \approx$ 0.001Å^{-1} to gain intensity. The crucial features in $R(q_z)$ can still be resolved. The main problem is the small sample size of 10 x 10 mm^2 where normally the illuminated area is at least 1 order of magnitude larger. The resulting reduced peak-to-background ratio of 3 to 4 orders of magnitude.

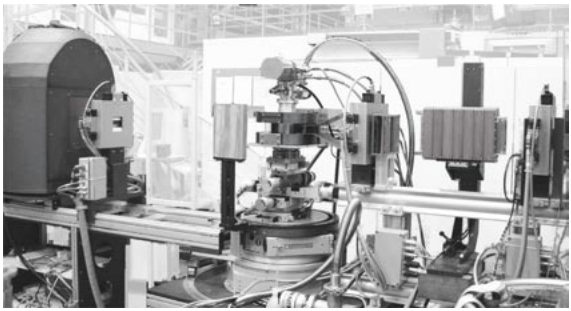

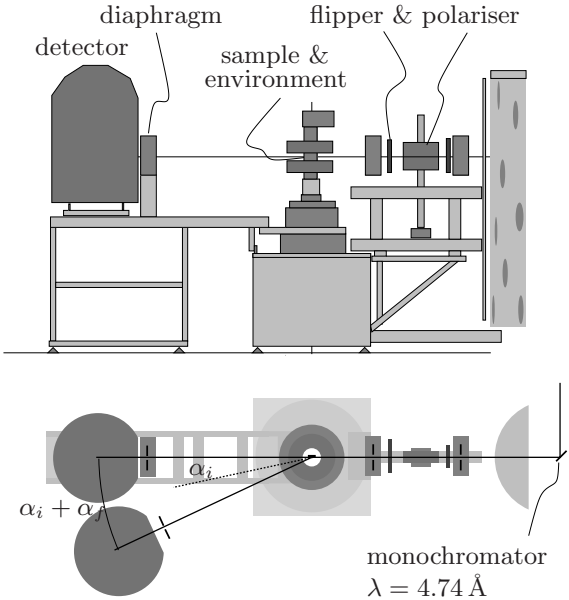

Figure 3: Experimental Setup on the angle dispersive neutron reflectometer Morpheus.

The intensity is measured as a function of incident and final angles, α_i and α_f while λ is kept constant. The sample is rotated relative to the neutron beam and the detector rotates around the sample by $\alpha_i + \alpha_f$.

The beam divergence is adjusted with diaphragms. Polarization is supplied by a magnetic supermirror polarizer, which is operated in transmission. The spin state can be changed by a flipper causing Larmor precession in a defined way.

A closed cycle refrigerator was used to vary the temperature of the sample between 10 K and 300 K. Magnetic fields up to 1000 Oe could be produced by a pair of Helmholtz coils surrounding the cooling device. The field direction is normal to the scattering plane and parallel to the sample surface.

Antiphase magnetic proximity effect

Fig. 4 shows typical $R(q_z)$ curves. The solid line represents the data obtained at room temperature. This temperature is above T_c and T_{curie} and therefore spin-up and spin-down neutrons see the same potential. The periodic structure of a multilayer leads to the Bragg condition for constructive interference (neglecting refraction) $\sin\alpha_i/\lambda = 1/2d$, with period d. In analogy to crystal reflections one thus speaks about Bragg peaks. The 1st Bragg peak is clearly visible, while the absence of the 2nd Bragg peak in the RT data is expected for a layer thickness ratio of 1:1 which leads to an extinction of all even Bragg peaks. The higher orders are already hidden in the background in this case.

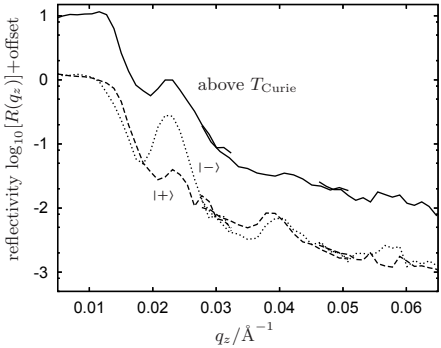

Figure 4: Reflectivity of a YBCO / LCMO multilayer at room temperature (*solid line, + 1*) and at T = 10K measured with spin up (*dashed*) and spin down neutrons (*dotted*).

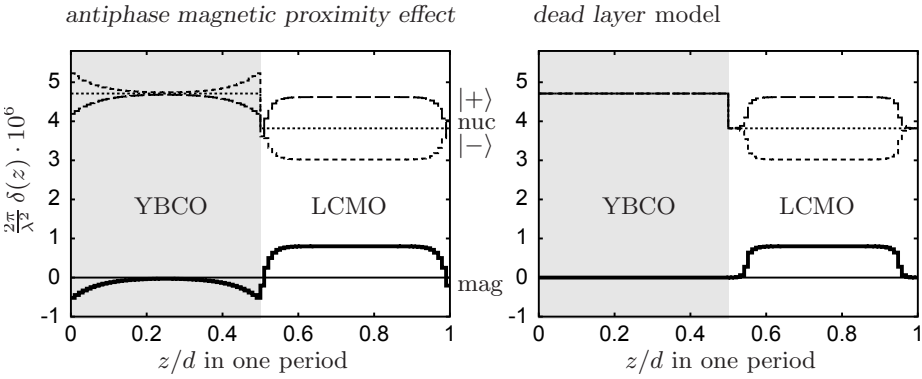

Figure 5: Schematic representation of the two models, which successfully describe the PNR data. The potentials for the nuclei, the magnetic induction and their sum / difference are drawn for one period of the superlattice.

The dashed lines represent data collected at 10 K, below T_c. Close to the critical edge the curves are shifted relative to the *RT* measurement. The reason is that the critical edge for total external reflection is proportional to V^2 of the top layer and thus increases (spin up) or decreases (spin down) for magnetic material.

Also the contrast between YBCO and LCMO is changed: it is reduced for spin up neutrons and enhanced for spin down neutrons. Therefore the intensity of the 1st Bragg peak decreases for spin up neutrons and increases for spin down neutrons. The same trend holds for the weakly visible 3rd Bragg peak.

The simplest model, which assumes a homogeneous magnetization of the LCMO layer and no magnetization in the YBCO layer, can not account for the existence of a 2nd order peak. Its appearance necessarily requires a magnetic induction profile that is shifted or not step-like at the interface. To pinpoint the detailed magnetization profile one has to perform computer simulations. For this we used the code EDXR [6].

As mentioned above this procedure will not give a unique solution. In our case quite a lot of models (exponential decay, magnetically dead layer, ...) reproduce the complete curve with the exception of the slight shift of the spin dependent 2nd order peaks relative to each other. Only two models were able to explain the data: a magnetically dead layer of 15 Å at the surface of LCMO, or a magnetic induction in YBCO with an exponential decay and an antiferromagnetic alignment to the induction in LCMO.

We were able to reproduce these main experimental results in all successive measurements on a number of different samples. Based on our PNR results alone we are not able to rule out one of the two models [5]. However, element specific XMCD measurements by J.,Chakhalian and coworkers [3] clearly reveal a magnetic moment on Cu, which is aligned antiparallel to the Mn moments. This observation is only consistent with the *antiphase magnetic proximity effect*.

Ambiguous role of superconductivity

So far we only discussed the magnetic induction profile at low temperature, *i.e.* well below T_c. Additional information can be obtained from the temperature dependence of $B(z)$. Fig. 6 shows $R(q_z)$ at $q_x \approx 0$ for various T. Two effects are visible: below T_{curie} the intensity of the 1st Bragg peak increases due to the increasing magnetization of the FM layers. The 2nd Bragg peak appears at about T=120 K, a temperature between T_c and T_{curie}.

If one takes into account the intensity scattered in the off-specular region ($q_x \neq 0$) also at T_c an effect can be seen (Fig. 7): At T_c the peak intensity has a maximum and then decreases again. Integration of the intensity over q_x includes the off-specularly scattered contributions, which results in a different temperature dependence: after renor-

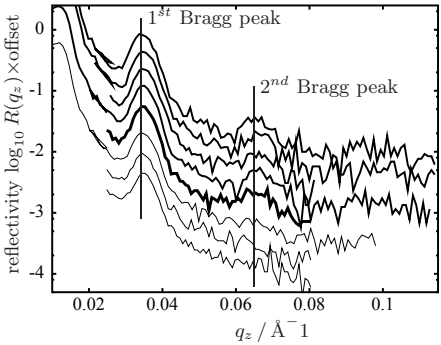

Figure 6: Unpolarized neutron reflectivity curves taken at temperatures between 200K (lowest curve) and 15K (top curve). Above T=120K (bold curve) no 2nd Bragg peak is visible, below its intensity is almost constant.

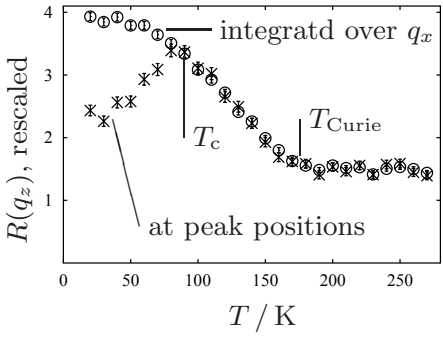

Figure 7: Intensities of the 1st Bragg peak from Fig. 6 as a function of temperature. *Crosses:* Intensity at the peak position for $q_x = 0$, *balls:* Intensity integrated over q_x, both scaled to the same value at $T>T_{Curie}$.

malization the second curve is identical to the first one down to T_c, but then it still increases slightly. This means that the magnetization in the FM layers still increases as expected for a pure FM, but the fact that it is scattered off-specular tells that at T_c some lateral magnetic inhomogeneities set in, which increase with decreasing temperature.

These inhomogeneities are most likely magnetic domain walls. Our data would then imply that the magnetic domains shrink in size below T_c and more domain walls are formed.

A mapping of the q_z, q_x plane (not shown) leads to the amazing result that these inhomogeneities are vertically coupled through the superconducting layers over at least a large fraction of the stack.

So far we have no definite explanation for the appearance of the 2nd Bragg peak at T'=120K. If the effect was related to superconductivity it should appear at the superconducting transition temperature T_c. We want to note, that superconducting fluctuations may well persist to temperatures far above T_c, as reported by [7]. Another prominent feature of the high T_c phase diagram is the existence of a normal state gap (pseudogap), which affects both the spin and charge degrees of freedom. Some theories link this effect to the formation of preformed pairs, which acquire the necessary phase coherence when the temperature is lowered to T_c. On the other hand if the magnetization of the interface was a pure magnetic effect, it should show up at T_{curie}.

Summary

The results of the measurements and their interpretation in terms of the magnetic profile can be summarized as follows:

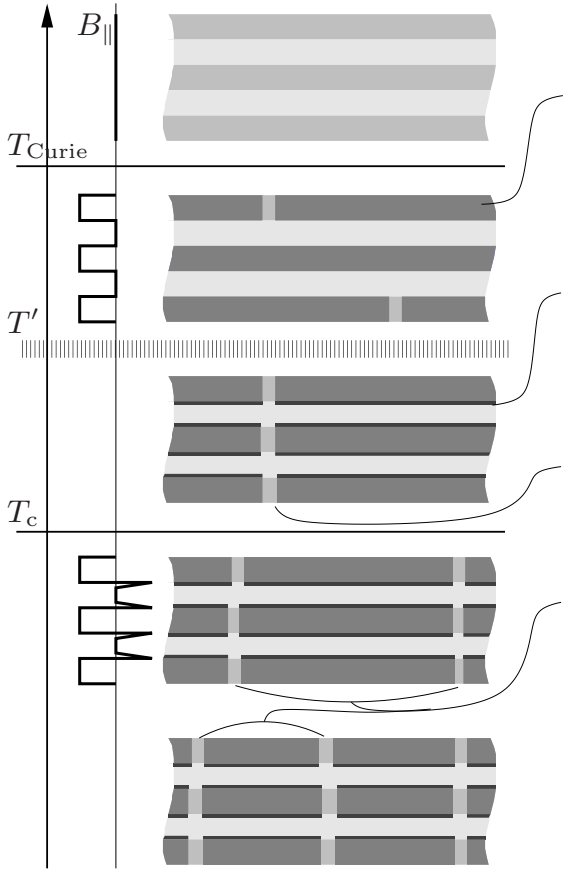

The ferromagnetic LCMO layers are magnetized in the same direction. No antiferromagnetic coupling of the layers is detected.

Interface effect of B(z) of the order of 10Å is measured at $T_c < T' \approx 140K < T_{Curie}$ *antiphase proximity effect* sets in

Simultaneous appearance of Bragg-sheets
Vertical correlation of magnetic domains

Increase of off-specular scattering below T_c
Shrinking of magnetic domains / characteristic length scale

Correlation of domain size with $T < T_c$ and XMCD measurements support the *antiphase proximity effect*

At present we do not have a complete physical picture that explains our experimental findings. There seems to be no direct connection between superconductivity and the *antiphase proximity effect*. One might speculate that this *new* phenomenon is related to the opening of a gap in the normal state (*pseudogap*). Further experiments on multilayers containing strongly underdoped YBCO layers may help to clarify this hypothesis.

References

[1] C. Niedermayer et al.: PSI Annual Report 2001, **1**

[2] J. Daillant, A.Gibaud: X-Ray and Neutron Reflectivity: Principles and Applications, Lecture notes in Physics, Springer (1998)

[3] J. Chakhalian et al.: Nature Physics **2**, 244-248 (2006).

[4] H.U. Habermeier et al.: Physica C **364-365**, 298 (2001).

[5] J. Stahn et al.: Phys. Rev. B **71**, 140509(R) (2005).

[6] P. Mikulík: EDXR - X-ray and neutron reflectivity calculation program, mikulik@physics.muni.cz

[7] V.J. Emery, S.A. Kivelson: Nature **374**, 434 (1995).

Host-Guest Interactions between Cellulose and Water

Ingo Grotkopp[1], Martin Müller[1], Fanni Juranyi[2]

[1]Institut für Experimentelle und Angewandte Physik, Universität zu Kiel, Leibnizstr. 19, D-24098 Kiel
[2]Laboratory for Neutron Scattering, PSI & ETH Zürich, 5232 Villigen PSI, Switzerland

Introduction

An enormous amount of empirical knowledge about woodworking has been collected during thousands of years. The properties of wood are highly influenced by its water content. The changes in the mechanics of wood due to water uptake, such as swelling and softening, are common knowledge. However, the mechanisms behind these effects are not always fully understood on the molecular level, and still further research is needed in this field.

Wood is a composite material that mainly consists of stiff cellulose crystals surrounded by a softer, water-adsorbing matrix. The structural changes present in wood under mechanical load can be monitored, in particular, it is possible to study the orientation and lattice spacing of the cellulose crystals by means of x-ray micro-diffraction with high spatial resolution [1-3]. However, it is necessary to investigate the structural changes as a function of the water content to clarify its influence. Additionally, the influence of wood on water is evident from trees surviving cold temperatures far below the freezing point of water. This effect is also of major interest for basic physical research and has been subject of several recent studies on water in confinement. Water adsorbed in the disordered regions of cellulose exhibits liquid dynamics below 0 °C and is therefore termed “non-freezing” [4]. Inelastic neutron scattering experiments can monitor such local dynamics of disordered material [5]. A refinement of this technique has been developed in order to enable such an investigation – despite the expected small signals – as a function of water content and of the orientation of the cellulose crystals [6].

Composite structure

Wood is a highly hierarchically structured material. If we look at the trunk of a felled tree, it has grown over several years which lead to the well-known annual rings in its

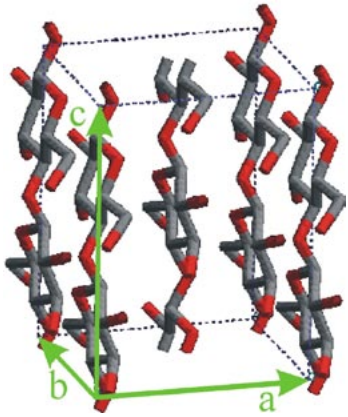

Figure 1: Unit cell of cellulose crystal type I_β. The carbon atoms are given in grey and the oxygen atoms in red. The fundamental vectors of the unit cell a, b, c are shown in green (see cover figure).

cross section. These rings consist of the cell walls from dead cells that had once been generated in the cambium of the tree. In the case of softwood, as for example pine, the structure is relatively simple. It consist of about 90 to 95 % of tracheids. These tracheids are long and slender cells and their longitudinal extension is aligned along the axes of the stem [7]p. 6. The high change in contrast at the ring boundary matches the beginning of a new year. The brighter band of the annual ring, which was produced in spring, is called earlywood. It consists out of thinner walls and larger cavities.

The growth process leads to a layered structure of the cell walls. The cellulose is polymerized by so-called terminal complexes during the life cycle of the cell, as recently reviewed in [8]. The cellulose chains are more or less well-ordered and aligned with respect to the main cell axis. The cellulose chains form small cellulose crystals, microfibrils, surrounded with some less ordered material. There are several crystal structures known for cellulose. Type I_β is the most abundant occurrence in plant cell walls and its unit cell is given in Figure 1. An accurate structure determination using x-ray and neutron diffraction can be found in [9].

Macroscopic Mechanical Properties and Crystal Orientation

The mechanical properties of wood are of major interest if it is used as building material. This is true in the case of the felled wood, when it is used for example to build structures as houses, as well as in the case of the living tree. Nevertheless, these two cases are different with respect to the water content of the wood. In the case of the living tree it is found to be between 30 and 220 wt% [10]Tab. 3-3. In the case of wood as an engineering material it is mostly used in a region below 15 wt%. of water [10]Fig. 9-4. This difference in moisture content has a huge influence on the mechanical properties of wood.

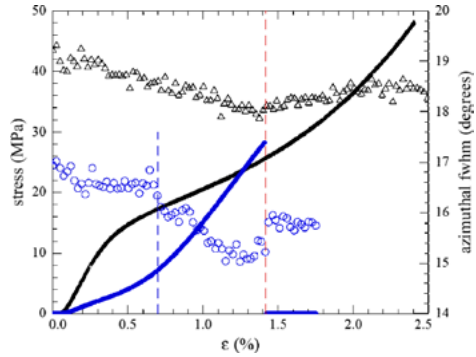

Figure 2: Macroscopic stress-strain curve and azimuthal width of the x-ray diffraction reflection of wet and dry pine earlywood.

The behaviour of condensed matter under mechanical load can be investigated on a macroscopic scale with simple experiments, where force and deformation are monitored over time. The tension case is of major interest for the living tree [11]Fig. 63.. Tensile tests on wood specimen have to be performed with respect to the fibre axis and the location of the annual rings. Hence, the samples investigated where chosen, to be small enough to consist of wood originating of only earlywood, taken from a tangential cut of a pine log.

The samples of about 40 mm length and 1 mm² cross section were stretched with a constant strain rate of 2 µm per second, i.e. 0.005 %/s, until fracture, in a combined stretching and x-ray diffraction experiment at HASYLAB. The influence of the moisture content is evident from Figure 2, where the macroscopic stress-strain curve and azimuthal width of the diffraction reflections are compared for typical wet and dry samples.

Inelastic Neutron Scattering Study

In models for water adsorption to cellulose, the water molecules are thought to be inserted between individual hydrogen bonded cellulose chains. Due to the anisotropic structure of the cellulose crystals the dynamics of such inserted water molecules might show a similar anisotropy. An investigation of oriented cellulose fibres, a model system for the composite material of the plant cell wall, with inelastic neutron scattering was performed to clarify this point.

The model system used was a bundle of flax fibres as shown in Figure 4. The inelastic neutron scattering experiment was carried out at "FOCUS" operating at 4 Å wavelength [12-15]. The orientation and moisture content of the sample were set during the experiment following the schedule given in Table 1. The sample was used in two dif-

Weight ± 0.5 mg	Removable water content	Orientation	Temperature ± 4 K	Label
79.5 mg	10.3 mg ± 1 mg 14.9 % ± 1 %	vertical	300 K	wet vertical 300 K
			180 K	wet vertical 180 K
		horizontal	300 K	wet horizontal 300 K
			180 K	wet horizontal 300 K
69.2 mg	0.0 mg ± 1 mg 0.0 % ± 1 %	vertical	300 K	dry vertical 300 K
			180 K	dry vertical 180 K
		horizontal	300 K	dry horizontal 300 K
			180 K	dry horizontal 180 K

Table 1: Schedule of the inelastic neutron measurements performed in the given order with a bundle of flax fibres.

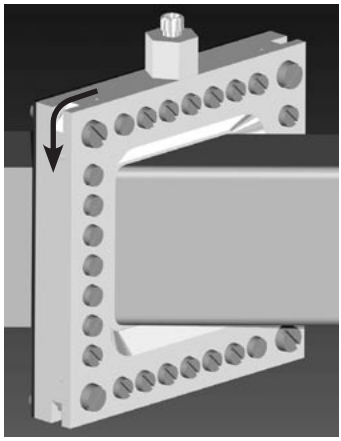

Figure 3: Sample container for orientation dependent neutron scattering experiments designed for the instrument "FOCUS". The green beam illustrates the path of incident and transmitted neutrons travelling from left to right. The four bigger screws at the corners are released to allow the rotation of the container by any multiple of 90°, as indicated by the red arrow. The small screws are used to hold the container sealed. The thread and hexagon at the top allows an easy connection to the instruments cryostat.

ferent orientations. In one case it was mounted in a way that the fibres were aligned horizontally, i.e. the fibres lie in the scattering plane defined by the middle detector bank of the instrument. In the other case the fibres were aligned vertically, i.e. with the fibre axis perpendicular to the scattering plane.

The diffraction patterns collected during the experiments reveal a good alignment of the fibre bundle and the cellulose crystals therein. The widths of the Bragg reflections are comparable to those found with x-ray diffraction at the same sample afterwards. No significant change in the width of the orientation distribution is visible throughout the experiments. A fit of a Gaussian profile (red curve) to the azimuthal distribution of the 200 reflection shows in all cases a full width at half maximum (FWHM) of about 22° and the orientation misalignment between wet and dry sample was no more than 2°.

The part of the spectroscopic information that was measured from the dry and wet samples can be easily compared when the corresponding signals are subtracted. This was performed for both orientations and two temperatures as shown in Figure 6. The signal shown here is that of all three detector banks of the instrument. The difference spectra obtained in this way are labelled "water", even though this signal

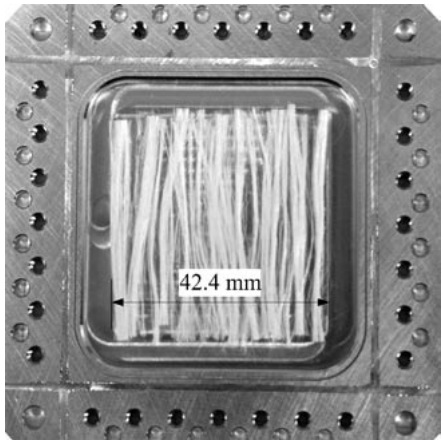

Figure 4: Bundle of flax fibres in the open sample container used in an inelastic neutron scattering experiment performed at FOCUS .

might not only be due to the dynamics of the adsorbed water but to a combination of the signal produced by the adsorbed water molecules and the changes in the cellulose. It is evident from Figure 6 that the adsorbed water causes a significant anisotropy in the region between 2 and 7 meV, even at 180 K, leading to a higher intensity for the horizontal orientation of the fibres. No significant change was observed for both orientations in the quasielastic region ± 1 meV around the elastic line. This energy range is linked to rotational and translational diffusion of water. Hence, motions in both directions are “equally populated” and indicate the frozen state at 180 K through their absence. A study on this signal for water in amorphous cellulose is given in [16].

There are at least two ways to explain the anisotropy in the dynamics observed in this study. First, the anisotropy can be linked to an anisotropy in the dynamics of the adsorbed water molecules only. Second, the dynamic response of the cellulose itself might have changed due to the presence of the adsorbed water molecules. It is known that the water molecules cannot penetrate into the cellulose crystals [17]. Therefore, a change in the dynamics originated directly to the dynamics of the water molecules must be located in the amorphous regions of the cellulose. This would imply an anisotropic environment of the water molecules, as is imaginable especially in the region close to the crystal surfaces.

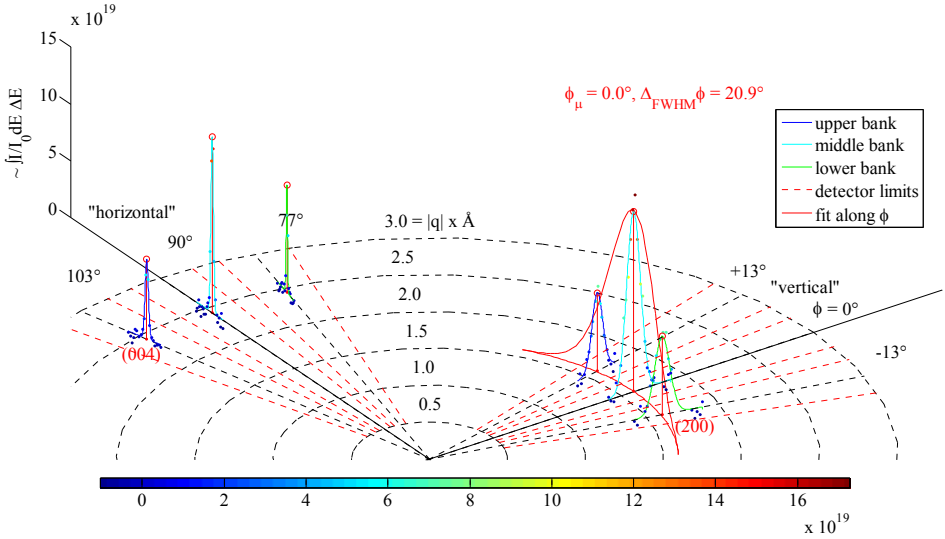

Figure 5: Diffraction pattern of the dry flax bundle at 180 K composed from the neutron scattering measurements of the horizontally and vertically aligned sample. The scattered points show the measured intensities colour-coded. The full lines represent the results of the fits to those points. The dashed red lines highlight the angular limits of the detectors used. The results of a Gaussian fit along the azimuth are shown in red. Details are given in the text.

Additionally, a change in the dynamics of the cellulose due to the water molecules can be a combination of two effects. It is conceivable that the hydroxyl groups at the surfaces of the crystals show a different response if water molecules are located in the vicinity of or even inserted into some of the hydrogen bonds between the crystals and the surrounding amorphous region, indicating a surface effect. Also it could be that the change in the dynamics is linked to a volume effect inside the crystals. This could be originating from a more smaller compressed lattice spacing, caused by the swelling of the amorphous regions at higher moisture content. Eventually, this effect could be limited to a few top most layers beyond the surface. Finally, the experimental findings might be a combination of all effects mentioned above.

Acknowledgement

The experiments that we presented above have been performed at large scale research facilities. Hence, we would like to thank the nearly infinite number of people that had been involved there. Without any order I would namely thank therefore Thierry Strässle, Andre Podlesnyak, Lothar Holitzner and Stefan Janssen from PSI and Sergio Funari and Martin Dommach from HASYLAB. It goes without saying, that a lot of financial support has been necessary to enable the presented research. Therefore, we express great thanks for foundation to the DFG (Mu 1673/3-1), the BMBF via the Saarland University, the HASYLAB (II-01-054, II-04-051) and the University of Kiel.

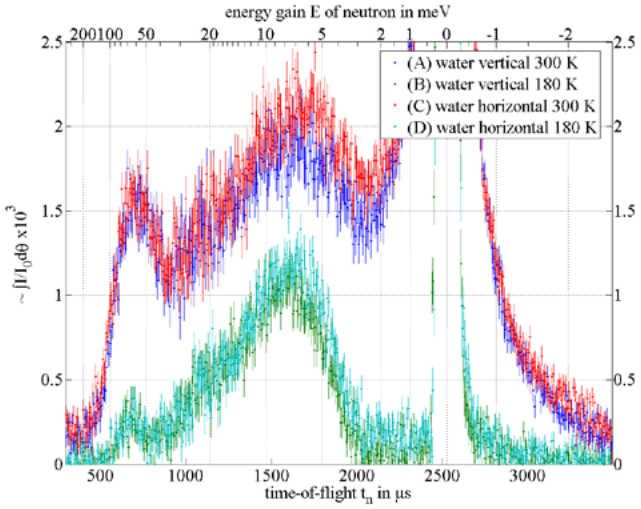

Figure 6: Differences of the intensity distributions collected in an inelastic neutron scattering experiment with a dry and a wet bundle of flax fibres integrated over all scattering angles shown against the time-of-flight of the scattered neutrons estimating the influence of the adsorbed water on the dynamics.

References

[1] Keckes, Jozef, Burgert, Ingo, Fruhmann, Klaus, Müller, Martin, Kölln, Klaas, Hamilton, Myles, Burghammer, Manfred, Roth, Stephan V., Stanzl-Tschegg, Stefanie, and Fratzl, Peter:
"Cell-wall recovery after irreversible deformation of wood";
Nature Materials; Vol. **2** (12), pages 810-814 (**2003**)
DOI: 10.1038/nmat1019

[2] Kölln, Klaas, Grotkopp, Ingo, Burghammer, Manfred, Roth, S. V., Funari, Sergio S., Dommach, Martin, and Müller, Martin:
"Mechanical properties of cellulose fibres and wood. Orientational aspects in situ investigated with synchrotron radiation";
Journal of Synchrotron Radiation; Vol. 12 (6), pages 739-744 (2005)
DOI: 10.1107/S0909049505011714

[3] Peura, M., Grotkopp, I., Lemke, H., Vikkula, A., Laine, J., Muller, M., and Serimaa, R.:
"Negative Poisson ratio of crystalline cellulose in Kraft cooked Norway spruce";
Biomacromolecules; Vol. **7** (5), pages 1521-1528 (**2006**)

[4] Czihak, Christoph Andreas:
"Cellulose: Structure and dynamics of a naturally occurring composite material as investigated by inelastic neutron scattering" (**2000**) Wien
Dissertation

[5] Müller, Martin, Czihak, Christoph, Schober, Helmut, Nishiyama, Yoshiharu, and Vogl, Gero:
"All disordered regions of native cellulose show common low-frequency dynamics";
Macromolecules; Vol. **33** (5), pages 1834-1840 (**2000**)
DOI: 10.1021/ma9912271

[6] Grotkopp, Ingo:
"Influence of Water on the Mechanical Properties of Wood - Investigated Using X-Ray and Neutron Scattering"
Mathematisch-Naturwissenschaftliche Fakultät der Christian-Albrechts-Universität (**2006**) Kiel
Dissertation

[7] Fengel, Dietrich and Wegener, Gerd:
"Wood: Chemistry, Ultrastructure, Reactions";
Walter de Gruyter, Berlin, New York, (**1984**)
ISBN: 3-11-008481-3

[8] Saxena, I. M. and Brown, R. M.:
"Cellulose biosynthesis: Current views and evolving concepts";
Annals of Botany; Vol. **96** (1), pages 9-21 (**2005**)
DOI: 10.1093/aob/mci15

[9] Nishiyama, Yoshiharu, Langan, Paul, and Chanzy, Henri:
"Crystal structure and hydrogen-bonding system in cellulose Iβ from synchrotron X-ray and neutron fiber diffraction";
Journal of the American Chemical Society; Vol. **124** (31), pages 9074-9082 (**2002**)
DOI: 10.1021/ja0257319

[10] Dietenberger, Mark A., Green, David W., Kretschmann, David E., Hernandez, Roland, Highley, Terry L., Ibach, Rebecca E., Liu, Jen Y., McDonald, Kent A., Miller, Regis B., Moody, Russel C., Rowell, Roger M., Simpson, William T., Soltis, Lawrence A., TenWolde, Anton, Wolfe, Ronald W., Vick, Charles B., White, Robert H., Williams, R. Sam, Winandy, Jerrold E., and Youngquist, John A.:
"Wood Handbook - Wood as an Engineering Material"
U.S. Department of Agriculture, Forest Service, Forest Products LaboratoryReport No. FPL-GTR-113, (**1999**)

[11] Mattheck, Claus and Kubler, Hans:
"Wood - The Internal Optimization of Trees";
Springer-Verlag, Berlin, Heidelberg, New York, (**1995**)

[12] Janssen, S., Mesot, J., Holitzner, L., Furrer, A., and Hempelmann, R.:
"FOCUS: A hybrid TOF-spectrometer at SINQ";
Physica B; Vol. **234-236**, pages 1174-1176 (**1997**)
DOI: 10.1016/S0921-4526(97)00209-3

[13] Janssen, S., Altorfer, F., Holitzner, L., and Hempelmann, R.:
"Time-of-flight spectrometer FOCUS at SINQ: first results";
Physica B; Vol. **276**, pages 89-90 (**2000**)
DOI: 10.1016/S0921-4526(99)01253-3

[14] Juranyi, F., Janssen, S., Mesot, J., Holitzner, L., Kagi, C., Tuth, R., Burge, R., Christensen, M., Wilmer, D., and Hempelmann, R.:
"The new mica monochromator for the time-of-flight spectrometer FOCUS at SINQ";
Chemical Physics; Vol. **292** (2-3), pages 495-499 (**2003**)
DOI: 10.1016/S0301-0104(03)00175-7

[15] Mesot, J., Janssen, S., Holitzner, L., and Hempelmann, R.:
"Focus: Project of a Space and Time Focussing Time-of-Flight Spectrometer for Cold Neutrons at the Spallation Source SINQ of the Paul Scherrer Institute";
Journal of Neutron Research; Vol. **3**, pages 293-310 (**1996**)

[16] Czihak, Christoph, Müller, Martin, Schober, Helmut, Heux, L., and Vogl, Gero:
"Dynamics of water adsorbed to cellulose";
Physica B; Vol. **266**, pages 87-91 (**1999**)

[17] Ioelovitch, M. and Gordeev, M.:
"Crystallinity of cellulose and its accessibility during deuteration";
Acta Polymerica; Vol. **45** (2), pages 121-123 (**1994**)
DOI: 10.1002/actp.1994.010450211

Announcements

SGN/SSDN Members

The Swiss Neutron Scattering Society welcomes the following new members:

- F. Mulhauser, Int. Atomic Energy Agency, Vienna
- H. Schober, Institut Laue Langevin, Grenoble
- U. Smirnova, University of Geneva
- O. Waldmann, University of Berne

Presently the SGN has 199 members.

SGN/SSDN online registration

Real online registration for new members of our society is now available from the SGN website. The former slightly "old-fashioned" application form has now been replaced by a professional online registration via the PSI Digital User Office system.

More information:

http://sgn.web.psi.ch
http://sgn.web.psi.ch/sgn/address_form.html

SGN/SSDN payment of member fees

The annual member fee of the SGN is very low (CHF 10,-) and is easily forgotten. As a reminder the *Swiss society members* will find a red "Einzahlungsschein" in this issue.

For the foreign members we tried to simplify the international bank transfer to the SGN bank account by printing the **IBAN and BIC code into the editorial**. In addition please find below the international coordinates of the SGN account:

Swiss Postfinance account: 50-70723-6,
BIC: POFICHBE, IBAN: CH3909000000050707236

Open Positions at ILL

To check the open positions at ILL please have a look at the ILL-homepage: http://www.ill.fr following the link 'Job Offers'.

News from PSI User Office

After the long break (the SINQ call for proposals in November 2005 was cancelled due to the extended shutdown 2006) the recent call for proposals in May 2006 was really successful: A total of 164 proposals were submitted, which is almost twice the result of previous calls.

The strongest request has been placed again for the SANS-instruments with 38 proposals followed by the two powder diffractometers DMC (24) and HRPT (22). Also the spectrometers like FOCUS (19) and TASP (18) are strongly requested by the user community. Regarding the number of requested days SANS-I (305) and TASP (211) take the lead.

Approximately 50% of the proposals were submitted by main-proposers from EC countries. From the scientific point of view 2/3 of the proposals belong to subcommittee I (Diffraction/Spectroscopy), 1/3 to subcommittee II (SANS/Reflectometry). All proposals have been handled by the Digital User Office, which allowed the upload of pdf-files for the first time. This option was well accepted by the authors (more than 50% of the proposals contain uploaded pdf-files).

The strong interest in the SINQ instruments is very encouraging for the team running the facility. It confirms that the instruments match quite successfully the demand of the user community. On the other hand it also means that quite a lot of proposals will have to be rejected not because of their missing scientific relevance but moreover due to the strong oversubscriptions. We hope not to discourage too many users this time and like to draw your attention already now to the next proposal submission deadline, which will be **November 15, 2006**.

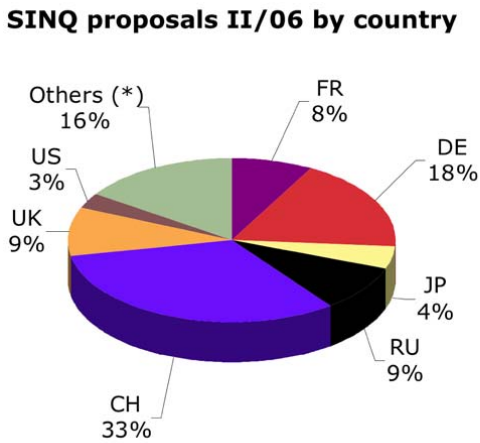

Figure 1: Submitted Proposals by country. (*) Others: 13 countries will less than 5 proposals each. In total the proposals were submitted from 20 different countries.

8th SINQ Users' Meeting

S. Janssen, PSI User Office, NUM department, Paul Scherrer Institute

On May 10, 2006 the 8th SINQ Users' Meeting was organized at the Paul Scherrer Institute (Villigen, Switzerland). Approximately 80 participants gathered at PSI for the one-day meeting to present their newest SINQ results and to receive latest information about the Swiss Neutron Source towards the end of the extended shutdown period in 2006.

Kurt Clausen, the director of the PSI department NUM 'Solid State Research with Neutrons and Muons' opened the meeting and welcomed the participants. He updated the audience about recent progress regarding the installation of the liquid metal MEG-APIE-target and presented the good news that the installation is still on schedule and the restart of SINQ is expected for the end of July. Afterwards the PSI general director Ralph Eichler welcomed the participants on behalf of the institute before Joël Mesot, head of the Laboratory for Neutron Scattering (PSI & ETH Zurich) gave some overview about both the in-house research at LNS and the instrumental upgrades, which will be available for the user operation in the future.

The scientific programme started with a talk from Barry Wells (Connecticut) about 'Electronic phase separation in superoxygenated $La_{2-x}Sr_xCuO_{4+y}$' followed by two presentations from Harald Schmidt (Clausthal) and Peter Lehmann (Lausanne) on

PSI director Ralph Eichler

Kurt Clausen, head of PSI NUM department

'Soft Condensed Matter' session

'Investigation of self diffusion in metastable solids with isotope multilayers and neutron reflectometry' and 'Soils, scales and structures - the application of neutron imaging in soil physics', respectively.

After the coffee break the audience split up to listen to two parallel sessions on 'Magnetism' and 'Soft Condensed Matter' with five and six presentations each. The afternoon programme consisted of two plenary sessions with a special emphasis on 'diffraction and materials' on the one hand and 'spectroscopy' on the other. In total 27 oral presentations were given. The programme of the meeting left also time for discussions among the participants or with the SINQ instrument responsibles. The poster session in the afternoon was just one opportunity for that.

The full programme of the meeting can be viewed following this link: http://sinq.web.psi.ch/sinq/usmeet_8/programme.html

Finally it is remarkable that an increasing number of presentations showed results that were obtained not only by neutron scattering experiments but also in combination with complementary experiments using X-rays at SLS or muons at SμS. This is a clear indication of the working concept to have three probes on one campus at PSI.

The next SINQ Users' Meeting will probably be organized in June 2007 in conjunction with the celebration of the 10th anniversary of SINQ.

Planning new experiments on FOCUS: Ingo Grotkopp (Kiel) and Thierry Straessle (LNS)

Barry Wells, University of Connecticut

Joël Mesot, Laboratory for Neutron Scattering, PSI & ETH Zürich

Coffee break!

Helmut Schober (ILL) listened to the users' meeting and later on presented the ILL news during the SGN general assembly.

Neutron, X-ray and Muon Studies of Nano Scale Structures

5th PSI Summer School on Condensed Matter Research
August 19–26, 2006, Lyceum Alpinum, Zuoz, Switzerland

Each summer PSI organises a summer school on a research theme where key new insight can be obtained through access to and use of its large scale research infrastructures. The topic for the 2006 school is: **Neutron, X-ray and Muon studies of nano scale structures** and will mainly focus on the study of soft matter systems. The school is addressed mainly to the education of PhD or postdoctoral students without prior knowledge of or experience with neutron, X-ray or Muon techniques. The school will start with 3 days of introduction to the techniques and conclude with a series of lectures providing an overview of state of the art in research using these techniques.
The school is open to the national and non-national public, the language of the school will be English.

Speakers include

K. Clausen, Villigen
S. Egelhaaf, Düsseldorf
T. Forsyth, Grenoble
M. Fuchs, Konstanz **
T. Gutberlet, Villigen
I.W. Hamley, Reading
J. Kohlbrecher, Villigen
E. Lehmann, Villigen
I. McKenzie, Stuttgart
J. Mesot, Villigen
K. Mortensen, Roskilde
F. Pfeiffer, Villigen
E. Pohl, Villigen
T. Prokscha, Villigen
L. Rivkin, Villigen
R. Scheuermann, Villigen
M. Stampanoni, Villigen
A. Stradner, Fribourg
D. Svergun, Hamburg
H. Vacklin, Oxford **
F. Van der Veen, Villigen
E. Windhab, Zürich **
R. Zorn, Jülich

** not yet confirmed

Organisation of the School

K.N. Clausen (Chairman), S. Janssen, R. Bercher (Secretary)

Program Committee

- Kurt Clausen, PSI, **chairman**
- Friso van der Veen, PSI
- Joel Mesot, PSI & ETHZ
- Dierk Herlach, PSI
- Rudolf Morf, PSI
- Stefan Janssen, PSI
- Renate Bercher, PSI, **school secretary**

Scientific advisory committee

- Michal Borkovec, University of Geneva, Switzerland
- Olwyn Byron, University of Glasgow, United Kingdom
- Jörg Löffler, ETH Zürich, Switzerland
- Kell Mortensen, Danish Polymer Centre, Denmark
- Dieter Richter, Forschungszentrum Jülich, Germany
- Emil Roduner, University of Stuttgart, Germany
- Louis Schlapbach, EMPA Dübendorf, Switzerland
- Peter Schurtenberger, University of Fribourg, Switzerland
- Fritz Winkler, Paul Scherrer Institut, Switzerland
- Hartmut Zabel, Ruhr-University Bochum, Germany

Residential accommodation will be available at the Lyceum Alpinum in Zuoz (costs: 800 Swiss Francs, including full board, banquet). The number of participants will be limited to 120. Closing date for Application is 30 June 2006.

For further information please contact
Renate Bercher, Paul Scherrer Institut, CH 5232 Villigen PSI,
Tel. +41 56 310 3402, Fax +41 56 310 3131,
email: Renate.Bercher@psi.ch, http://num.web.psi.ch/zuoz2006/

PL607_03.06 / bx91

Conferences and Workshops 2006/2007

(an updated list with online links can be found here:
http://sinq.web.psi.ch/sinq/links.html)

July 2006

XVIII International School on Physics and Chemistry of Condensed Matter: Spectroscopy of Modern Materials
July 1-8, 2006, Bialowieza, Poland

Strongly Correlated Systems in Low Dimension
July 2-8, 2006, Ascona, Switzerland

XIV Congress - Italian Society of Synchrotron Light (SILS)
July 6-8, 2006, Napoli, Italy

XIII International Conference on Small Angle Scattering
July 9-13, 2006, Kyoto, Japan

M2S-HTSC-VIII, 8th International Conference on Materials and Mechanisms of Superconductivity and High Temperature Superconductors
July 9-14, 2006, Dresden, Germany

International Workshop on Nanospectroscopy using Synchrotron Radiation
July 12-14, 2006, PSI Villigen, Switzerland

Workshop Neutrons for Geoscience
July 14, 2006, FRM-II Garching, Germany

15th International Conference on Solid Compounds of Transition Elements
July 15-20, 2006, Krakow, Poland

ACA 2006, Annual Meeting of the American Crystallographic Association 2006
July 22-27, 2006, Honolulu, Hawaii, USA

SRMS-5, Fifth International Conference on Synchrotron Radiation in Materials Science
July 30 - August 2, 2006, Chicago IL, USA

ICN+T 2006: International Conference on Nanoscience and Technology
July 30 - August 4, 2006, Basel, Switzerland

August 2006

ISIS Excitations User Group Meeting
August 2, 2006, The Cosenor's House, Abingdon, United Kingdom

Theoretical and Experimental Magnetism Meeting
August 3-4, 2006, The Cosenor's House, Abingdon, United Kingdom

ECM23: 23rd European Crystallographic Meeting
August 6-11, 2006, Leuven, Belgium

National School on Neutron and X-ray Scattering
August 13-27, 2006, Argonne National Laboratory, IL, USA

Highly Frustrated Magnetism 2006
August 15-19, 2006, Osaka, Japan

5th PSI Summer School on Condensed Matter Research
August 19-26, 2006, Zuoz, Switzerland

International Conference on Magnetism 2006
August 20-25, 2006, Kyoto, Japan

Siena 2006: IUCr School on Basic Crystallography
August 27 - September 2, 2006, Siena, Italy

International Conference on Electronic Spectroscopy and Structure
August 28 - September 1, 2006, Foz do Iguacu, PR, Brazil

Workshop on Nano-materials and Powder Diffraction
August 31, 2006, Geneva, Switzerland

Workshop on Pharmaceutical Applications of X-Ray Powder Diffraction
August 31, 2006, Geneva, Switzerland

International Summer School on Neutron Techniques in Molecular Magnetism
August 31 - September 9, 2006, Jaca, Spain

September 2006

One day ‚Under the Bonnet' Powder Diffraction Software Workshop
September 1, 2006, Geneva, Switzerland

10th European Powder Diffraction Conference
September 1-4, 2006, Geneva, Switzerland

IC fe 2006: 6th International Conference on f-elements
September 4-9, 2006, Wroclaw, Poland

EMPG XI: Mineralogy, Petrology and Geochemistry
September 11-13, 2006, Bristol, United Kingdom

2nd MaNEP Summer School: Probing the physics of low dimensional Systems
September 11-16, 2006, Saas Fee, Switzerland

2006 Test, Research and Training Reactor Conference
September 12-15, 2006, Austin, Texas, USA

7th European Conference on Residual Stresses
September 13-15, 2006, Berlin, Germany

Polarised Neutron School
September 19-22, 2006, Berlin, Germany

PNCMI 2006, Polarised Neutrons in Condensed Matter Investigations
September 25-28, 2006, Berlin, Germany

School of Neutron Scattering Francesco Paolo Ricci: Structure and Dynamics of Magnetic Systems
September 25 - October 6, 2006, Santa Margherita di Pula, Sardegna, Italy

Synchrotron Radiation in Art and Archaeology
September 27-29, 2006, Berlin, Germany

7th SLS Users' Meeting
September 28-29, 2006, PSI Villigen, Switzerland

Crystallography at High Pressures 2006
September 28 - October 1, 2006, Dubna, Russia

WINS 2006: 3rd Workshop on Inelastic Neutron Spectrometers 2006
September 29-30, 2006, Berlin, Germany

October 2006

International Workshop on Applications of Advanced Monte Carlo Simulations in Neutron Scattering
October 2-4, 2006, PSI Villigen, Switzerland

German Conference for Research with Synchrotron Radiation, Neutrons and Ion Beams at Large Facilities 2006
October 4-6, 2006, Hamburg, Germany

4th General NMI3 Meeting
October 9-11, 2006, Taormina, Sicily, Italy

EMBO Practical course on Solution Scattering from Biological Macromolecules
October 23-30, 2006, EMBL Hamburg, Germany

November 2006

Workshop on Future Developments of European Muon Sources
November 2-3, 2006, The Cosenor's House, Abingdon, United Kingdom

ICSFS-13, International Conference on Solid Films and Surfaces
November 6-10, 2006, San Carlos de Bariloche, Patagonia, Argentina

ILL Soft Matter User Meeting
November 22-24, 2006, Grenoble, France

December 2006

2nd IEEE International Conference on e-Science and Grid Computing
December 4-6, 2006, Amsterdam, Netherlands

March 2007

NOP 07: European Workshop on Neutron Optics
March 5-7, 2007, PSI Villigen, Switzerland

June 2007

Engineering of Crystalline Materials Properties: State-of-the-Art in Modeling, Design, and Applications
June 7-17, 2007, Erice, Italy

ECNS 2007: 4th European Conference on Neutron Scattering
June 25-29, 2007, Lund, Sweden

August 2007

ECM24: 24th European Crystallographic Meeting
August 22-27, 2007, Marrakech, Morocco